

Supplementary Materials for

Macrophage activation on “phagocytic synapse” arrays: Spacing of nanoclustered ligands directs TLR1/2 signaling with an intrinsic limit

Miao Li, Haomin Wang, Wenqian Li, Xiaoji G. Xu, Yan Yu*

*Corresponding author. Email: yy33@indiana.edu

Published 2 December 2020, *Sci. Adv.* **6**, eabc8482 (2020)
DOI: [10.1126/sciadv.abc8482](https://doi.org/10.1126/sciadv.abc8482)

This PDF file includes:

Figs. S1 to S9

Supplementary Figures

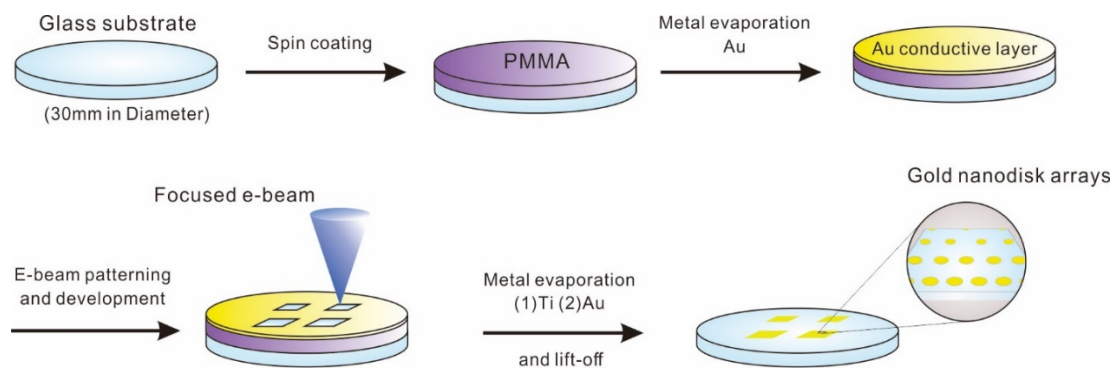


Fig. S1. Schematic illustration of processing flow of nanoarray fabrication. A single resist layer poly (methyl methacrylate) (PMMA) was spin-coated onto a clean glass substrate. A thin layer of Au (6 nm) was further coated on top of PMMA for conductivity. After electron beam patterning and wet solvent development, the glass substrate was coated sequentially with a titanium (Ti) adhesion layer (15 nm) and a gold (Au) surface layer (30 nm). The nanodisk arrays on the substrate were generated by lift-off in acetone.

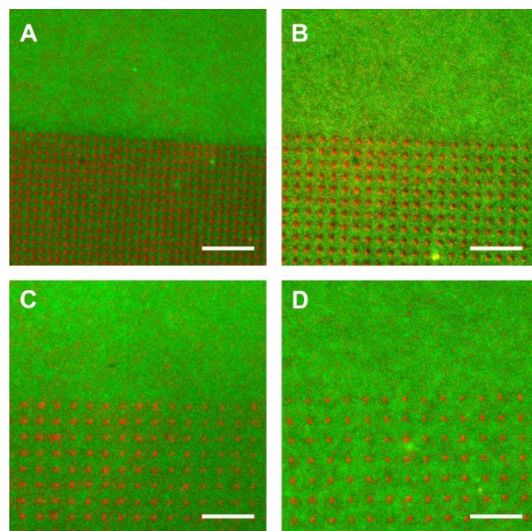


Fig. S2. Fluorescence images of the bifunctionalized nanoarrays with various inter-disk spacings: 1.0 μm (A), 1.5 μm (B), 2.0 μm (C) and 2.5 μm (D). Rhodamine-labeled Pam₃ (shown in red) was conjugated onto the gold nanodisks and Alexa Fluor 488-labeled IgG (shown in green) was conjugated on the surrounding glass substrates (Scale bars: 10 μm)

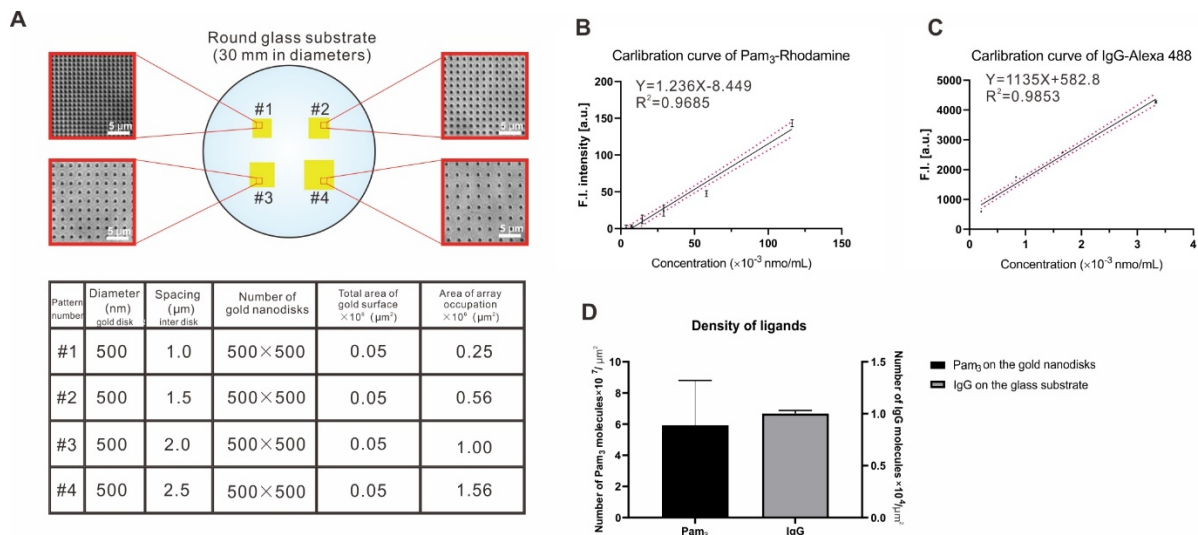


Fig. S3. Quantification of conjugation density of Pam₃ and IgG on the nanoarrays. (A) Geometric parameters of the gold nanodisk arrays. On a single glass substrate, four types of nanoarrays (inter-disk spacing 1.0, 1.5, 2.0, and 2.5 μm) were fabricated with the same number of the gold nanodisks (500 by 500) and the same diameters of individual gold nanodisk (500 nm). (B-C) Calibration curves of fluorescence intensities of Rhodamine-Pam₃ (Ex./Em. 549/578) and Alexa Fluor 488-IgG (Ex./Em. 488/525) as a function of concentration in bulk solutions. Each data point represents ave. ± s.d. obtained from three independent measurements. Solid lines indicate the linear fit and dashed lines indicate the 95% confidence intervals. (D) The estimated conjugation densities of Pam₃ and IgG on the gold nanodisks and surrounding glass surface, respectively. Bar plots represent ave. ± s.d. obtained from three independent measurements.

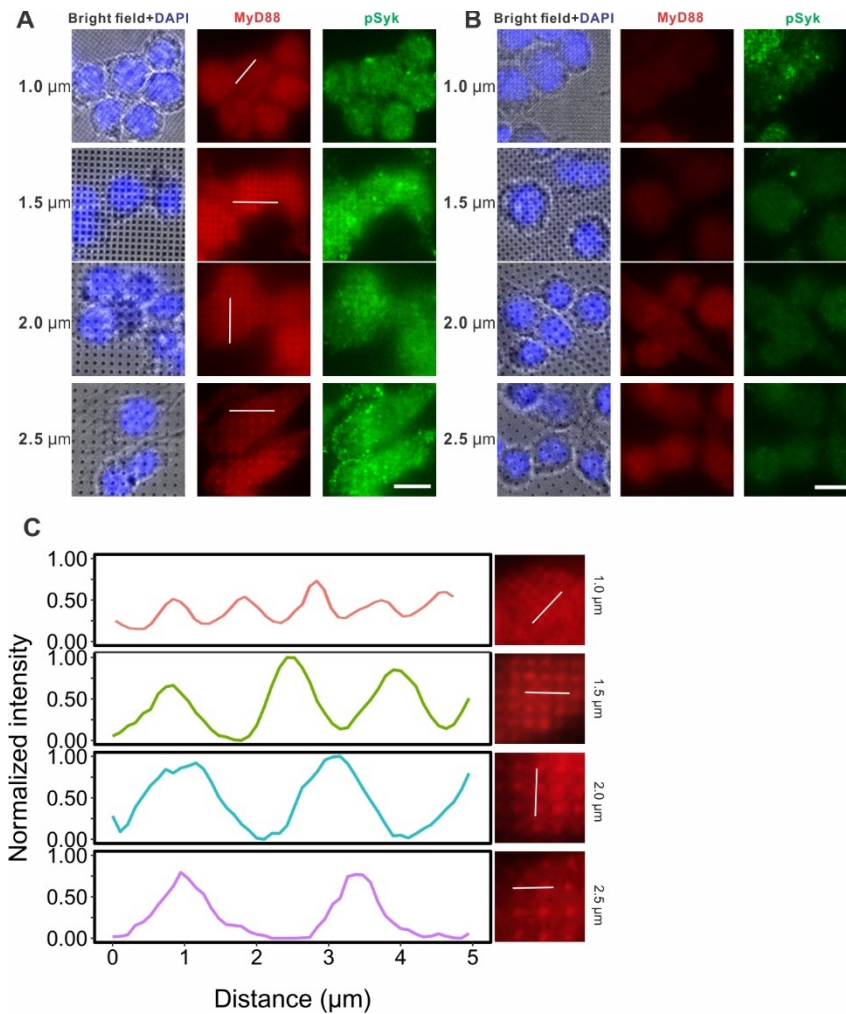


Fig. S4. Receptor activation and spatial organization on nanoarrays. (A-B) Representative bright-field and fluorescence images of RAW 264.7 macrophage cells that were immunostained for MyD88 (red), pSyk (green) and nucleus (blue) on the nanoarrays with (A) and without (B) Pam₃+IgG functionalization (Scale bar: 10 μm). (C) Fluorescence intensity line plot of MyD88 foci on the indicated nanoarrays.

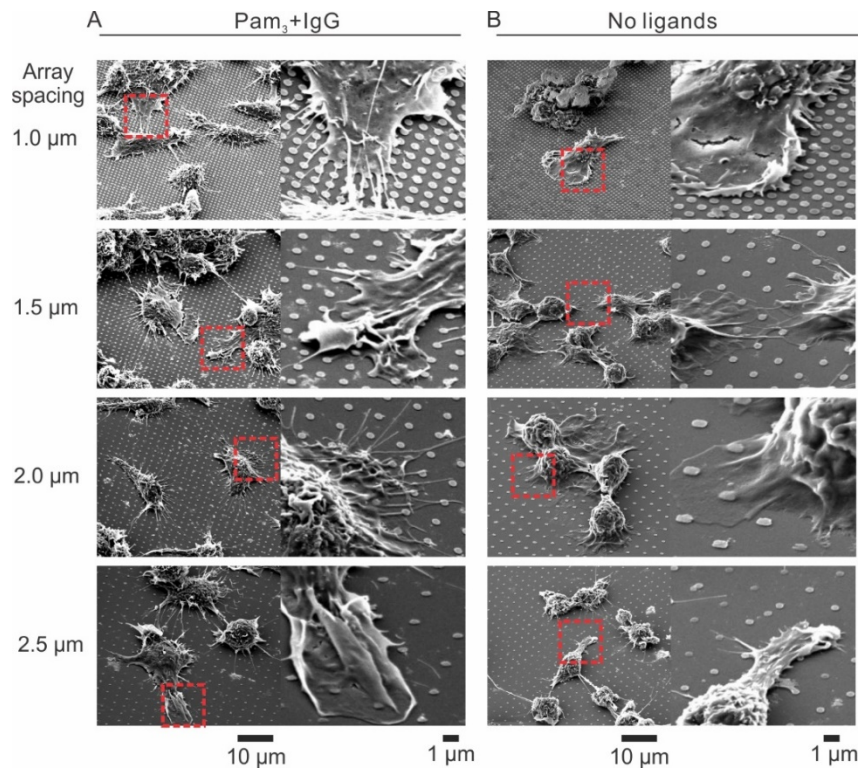


Fig. S5. SEM images of cell morphology on patterned substrates: (A) Cells on nanoarrays functionalized with Pam3 and IgG. (B) Cells on nanoarrays without ligands.

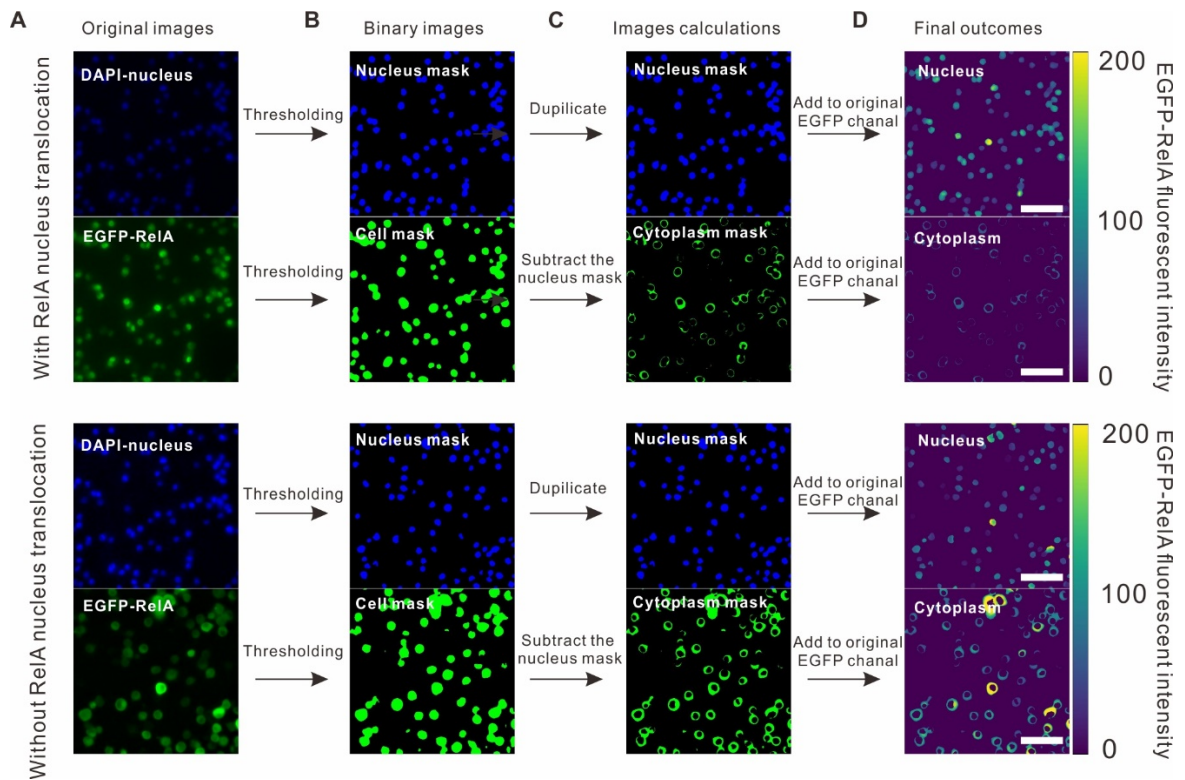


Fig. S6. Processing flowchart of image analysis of NF- κ B RelA nuclear translocation. (A) RAW264.7 cells stably expressing EGFP-RelA were stained with Hoechst 33342 and imaged in both GFP and DAPI channels. (B) The original fluorescence images were converted to binary images using automatic local thresholding. (C) The images at DAPI channel were used as the nuclear mask; the cytoplasmic mask was obtained by subtracting the nuclear mask from the cell mask. (D) The nuclear and cytoplasmic masks, respectively, were applied to the original EGFP-RelA images, to obtain the separated nuclear and cytoplasmic fluorescence images. (Scale bars: 40 μ m)

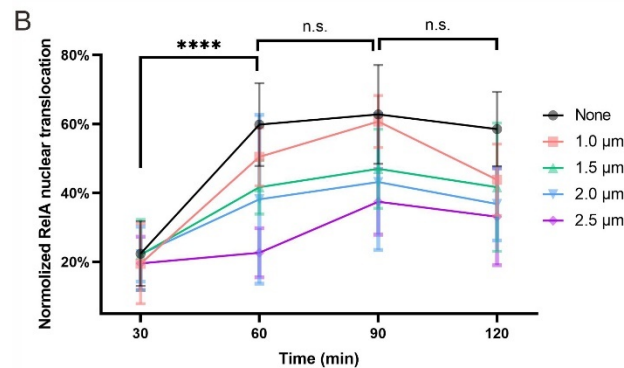
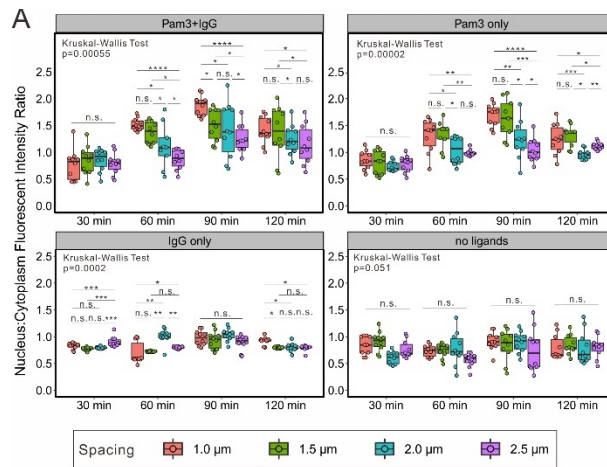


Fig. S7. Quantification of NF- κ B RelA nuclear translocation. (A) The time- and spacing-dependent NF- κ B RelA nuclear translocation of macrophages growing on indicated nanoarrays. Data are presented as box-and-whisker plots plus individual points overlay. Each point represents the average value of nucl:cyto fluorescent intensity ratio from one image containing ~ 50 cells. Statistical significance, assessed using Kruskal-Wallis test with Dunn's test as a post-hoc tests for multiple-group comparisons, is highlighted by P values as follows: ns $p > 0.05$, * $p \leq 0.05$, ** $p \leq 0.01$, *** $p \leq 0.001$, **** $p \leq 0.0001$. **(B)** Line plots showing the NF- κ B normalized cytoplasm-to-nucleus translocation ratio (ave. \pm s.d) as a function of activation time on different types of substrates as indicated. "None" indicates non-patterned substrates coated with ligands Pam3 and IgG.

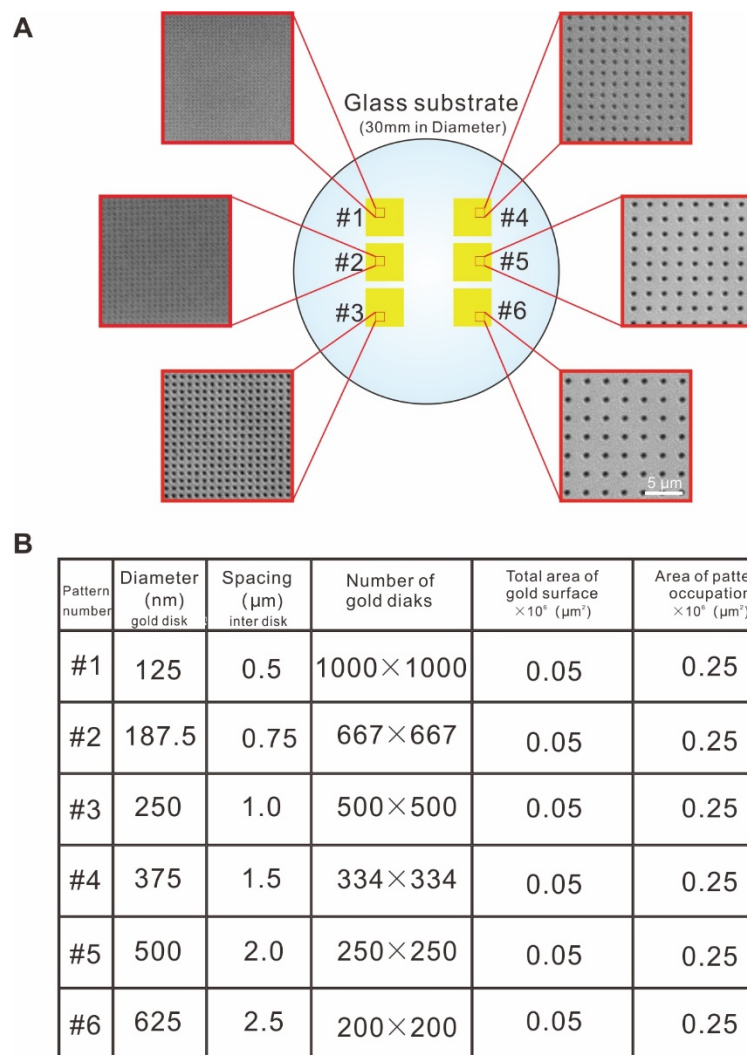


Fig. S8. Design of modified nanoarrays that vary in spacings but present the same amount of Pam3 and IgG per unit surface area. (A) Schematic illustration and the bright-field images of nanoarrays with various gold nanodisks spacings whilst keeping the same total gold surface areas within a given region. **(B)** Geometric parameters of each type of gold nanodisk arrays.

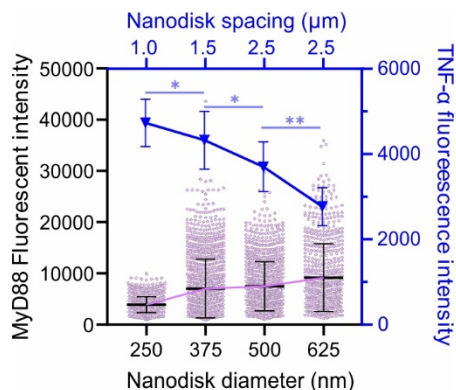


Fig. S9. Plots showing fluorescence intensity of immunostained MyD88 on individual gold nanodisks and average intracellular TNF- α levels (blue) in cells. X-axes indicate nanodisk diameter and corresponding spacing. For MyD88 data, each point represents a readout on a single nanodisk and each group of data is presented as ave. \pm s.d. plus individual points overlay. For 1.0 μm : n = 1109 disks; 1.5 μm : n = 1287; 2.0 μm : n = 1125 and 2.5 μm : n = 705. TNF- α data presented here are the same as in Fig. 6D. and presented as ave. \pm s.d.. Each data point of TNF- α intensity result is from 10 images containing n cells: n = 257 cells (0.5 μm), 184 (0.75 μm), 242 (1.0 μm), 281 (1.5 μm), 357 (2.0 μm), 288 (2.5 μm). Statistical significance, assessed using Kruskal-Wallis test with Dunn's test as a post-hoc tests for multiple-group comparisons, is highlighted by P values as follows: *p \leq 0.01, **p \leq 0.01.